Hindawi Publishing Corporation
Journal of Nanomaterials
Volume 2015, Article ID 210734, 8 pages
http://dx.doi.org/10.1155/2015/210734

Research Article

Silver Nanoparticles Influence on Photocatalytic Activity of Hybrid Materials Based on TiO_2 P25

Tomkouani Kodom,[1,2] Edina Rusen,[1] Ioan Călinescu,[1] Alexandra Mocanu,[1] Raluca Şomoghi,[3] Adrian Dinescu,[4] Aurel Diacon,[1] and Cristian Boscornea[1]

[1]*Department of Bioresources and Polymer Science, University Politehnica of Bucharest, 1-7 Gh. Polizu Street, 011061 Bucharest, Romania*
[2]*Laboratory of Water Chemistry, Faculty of Sciences, University of Lomé, Lomé, Togo*
[3]*National Research and Development Institute for Chemistry and Petrochemistry (ICECHIM), 202 Independence Street, District 6, CP 35-174, 060021 Bucharest, Romania*
[4]*National Institute for Research and Development in Microtechnologies (IMT-Bucharest), 126 A, Erou Iancu Nicolae Street, P.O. Box 38-160, 023573 Bucharest, Romania*

Correspondence should be addressed to Cristian Boscornea; boscornea_cristian@yahoo.com

Received 13 September 2014; Revised 17 December 2014; Accepted 18 December 2014

Academic Editor: Ping Xu

The aim of the present study consists in the obtaining of a hybrid material film, obtained using TiO_2 P25 and silver nanoparticles (AgNPs). The film manufacturing process involved realization of physical mixtures of TiO_2 P25 and AgNPs dispersions. The size distribution of the AgNPs proved to be a key factor determining the photodegradation activity of the materials measured using methyl orange. The best result was 33% degradation of methyl orange (MO) after 150 min. The second approach was the generation of AgNPs on the surface of TiO_2 P25. The obtained hybrid material presents photocatalytic activity of 45% MO degradation after 150 min. The developed materials were characterized by UV-VIS, SEM, and DLS analyses.

1. Introduction

One of the most omnipresent problems affecting people throughout the world is inadequate access to clean water and sanitation. Problems with water are expected to increase over the next decades, with water insufficiency occurring globally, even in regions currently assigned as water-rich [1, 2].

TiO_2 is the most commonly used oxide semiconductor in numerous fields (white pigments, dyes, and coatings, cosmetics, food, bleaching products, and solar cells) [3] which proved to be an ideal photocatalyst due to its ability to completely mineralize the target pollutants from wastewaters into H_2O and CO_2 [4]. Although TiO_2 is abundant, cost-effective, environmentally friendly, and photochemically stable under severe conditions [5], it has several disadvantages. One of these is related to the wide bandgap energy of 3.0 eV for rutile, respectively, and 3.2 eV for anatase which limits its applications, making possible the utilization of only 5% of the solar spectrum [1]. Furthermore, the high dispersion in water that causes sedimentation difficulties and sensitivity to the recombination of photoinduced electrons and holes also decreases its photocatalytic activity. Nevertheless, many studies have been reported using TiO_2 as photocatalyst for wastewater treatment against organic pollutants and pathogens [6–8]. The photocatalytic tests use TiO_2 as powder suspension or as thin films immobilized on different substrates. The major drawback of the TiO_2 powder dispersed in suspension systems is represented by the filtering expensive process necessary for the TiO_2 recovering [4, 9, 10]. Degussa P25 is a product commercially available in the market and represents one of the most used forms of TiO_2 composed of 70–80% anatase and 20–30% rutile crystallites with an average particle size of 25 nm. Degussa P25 is commonly used as a standard reference photocatalyst in order to compare the photocatalytic activity with other photocatalysts [4].

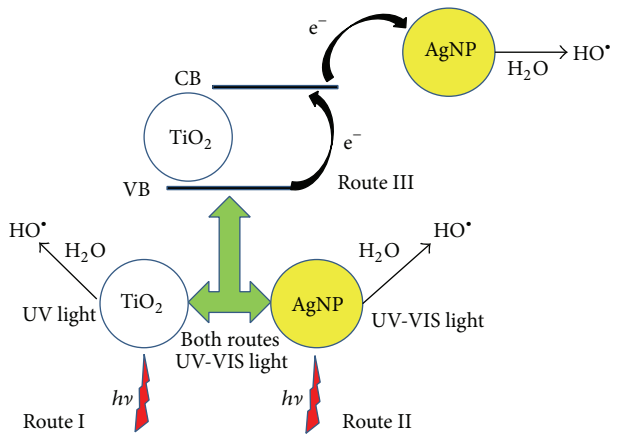

Scheme 1: Possible routes for the photoactivity of TiO_2 AgNPs hybrid materials.

The TiO_2 photodegradation mechanism can be explained by the promotion of an electron in the conduction band (CB) under UV light resulting in a "hole" in the valence band (VB) and the formation of electron-hole (e^--h^+) pairs. After losing the electron, the hole tries to recover the electron deficiency from the conduction band (recombination) or from the water adsorbed on the material's surface. The interaction with water leads to the formation of hydroxyl radicals ($HO^\bullet$) which are able to oxidize any organic compound and finally to CO_2 and water [1, 7]. The electron from the CB has no hole to initiate the recombination process; thus the most rapid alternative to reduce is to form the superoxide radical anion ($^\bullet O_2^-$) by reducing the oxygen adsorbed at the TiO_2 surface. The superoxide anion reacts with water to form more $HO^\bullet$ [7, 11].

The performance of TiO_2 based photocatalysts can be enhanced by doping with noble metals (Au, Ag, and Pt) [12] or several semiconductor compounds (In_2O_3, Cu_2S, CdTe, and NiO) [13–15] that improve the sensitivity of TiO_2 to visible light. Recent studies revealed that silver and silver nanoparticles (AgNPs) improve the photocatalytic activity of TiO_2 [16, 17] inducing an efficient surface plasmon resonance effect under sunlight preventing the recombination of e^--h^+ pairs responsible for the decreasing process of the photocatalytic activity of TiO_2 [18, 19].

Therefore, the TiO_2/AgNPs hybrid materials can be activated for water disinfection and photodegradation by both UV and visible light based on three possible routes (Scheme 1) that associate the photocatalytic properties of TiO_2 (route I) with the antimicrobial and photocatalytic characteristics of AgNPs (route II) [17, 20] and the interaction between TiO_2 and Ag (route III).

In this study, two methods were employed to obtain TiO_2 films doped with AgNPs with enhanced photoactivity. The first approach involved the synthesis of AgNPs solutions which were then used for realization of TiO_2 P25 dispersions in order to obtain films on a quartz tube followed by annealing. The size distribution influence on the enhancement of the photocatalytic activity was investigated. The second approach was aimed at simplifying the doping procedure. Thus, the manufacturing process consisted in the generation of AgNPs directly on the surface of TiO_2 P25 films and sinterization. The photodegradation activity of the films was investigated using methyl orange (MO) as target organic compound and TiO_2 as reference.

2. Experimental Procedures

2.1. Materials. $AgNO_3$ (ACS, Sigma-Aldrich), sodium borohydride ($NaBH_4$, Sigma-Aldrich), trisodium citrate dihydrate (Sigma-Aldrich), titanium dioxide (TiO_2 P25) (Degussa), methyl orange (MO) (Sigma-Aldrich), and acetic acid (Fluka) were used as received.

2.2. Methods

2.2.1. Ex Situ AgNPs Samples Synthesis (A, B, and C). 0.075 g (0.44 mmoles) $AgNO_3$ was dissolved in 200 mL ultrapure water in a round bottom flask maintained at 5°C. To this mixture, 0.4 g (1.36 mmoles) trisodium citrate dihydrate was added and the solution was stirred for 5 minutes, after which a solution of $NaBH_4$ (0.294 mmol/L) was introduced dropwise as follows in three different experiments: 0.3 mL (resulting sample A), 1.5 mL (resulting sample B), and 4 mL (resulting sample C), and the mixture was stirred for 30 minutes. The resulting AgNPs were used for the realization of the TiO_2 dispersions.

2.2.2. TiO_2 P25 Ex Situ AgNPs Film Realization. The TiO_2 P25 and TiO_2 P25/AgNPs films realization steps consist in the obtaining of stable dispersions, dip-coating of the quartz tube, and annealing at 500°C for 2 h.

3 g of TiO_2 P25 was well dispersed in 60 mL of AgNPs solution (A, B, or C) using an ultrasonic processor. The pH of the dispersion was adjusted to 4 using concentrated acetic acid.

For the reference TiO_2 P25 film ultrapure water was used for the realization of the dispersion and acetic acid for pH control. Prior to film deposition, the quartz tube was hydrophilized by immersion in a 5% NaOH solution overnight followed by rinsing with ultrapure water.

2.2.3. TiO_2 P25 AgNPs on Surface Generation. After obtaining by dip coating the TiO_2 P25 film on the quartz tube, the film was dried in oven at 80°C for 2 h and then immersed in solution A containing $AgNO_3$ (0.221 mmol/L) for 8 minutes after which it was introduced in solution B containing trisodium citrate (0.775 mmol/L) and $NaBH_4$ (0.0126 mmol/L). The obtained yellowish film is then sinterized in an oven at 500°C for 2 h.

2.3. Characterization. UV-VIS absorption spectra were recorded with an Able Jasco V-550 spectrophotometer; for the solid samples, reflection spectra were registered using an integrating sphere at normal incidence, a band width of 1 nm, and a scanning speed of 1000 nm min^{-1}.

The particle size measurement, through dynamic light scattering (DLS), was realized using a Nani ZS device (redbadge).

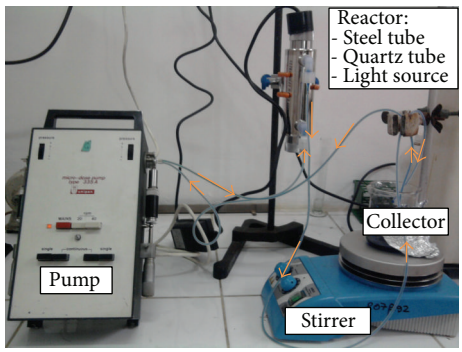

Scheme 2: The experimental set-up used for photocatalytic degradation.

For the morphological characterization of the obtained TiO_2 and TiO_2 AgNPs films scanning electron microscopy analyses were performed using a FE-SEM (field emission-scanning electron microscope) RAITH e_Line at 10 kV acceleration voltage. The AgNPs morphology was investigated by TEM using a high resolution transmission electron FEI Tecnai F30 S-Twin microscope. A drop of the AgNPs suspension was mounted on a holey carbon film copper grid allowing the solvent to evaporate at room temperature.

2.4. Photodegradation Procedure. The photodegradation measurements were analyzed using a modified commercial set-up comprised of (a picture of the set-up is presented in Scheme 2):

(i) microdosing pump Masterflex-Unipan 335 A with a flow fixed at 350 mL/h,

(ii) stainless steel jacket (21 cm) with a quartz tube core (used for photoactive material deposition) (the space between the jacket and the tube (180 cm^3) was used for the dye solution circulation),

(iii) UV-C lamp introduced inside the quartz tube (λ = 253.7 nm, power 4 W),

(iv) collecting flask used as starting and end point for the dye solution,

(v) silicon tubing connections used for connecting the collecting flask, pump, and reactor.

For the photodegradation studies, 200 mL MO with a concentration of 0.5 mol/L was utilized.

3. Results

In order to obtain hybrid nanomaterials with photocatalytic activity, the first step was to synthesize different AgNPs and characterize their behavior. In Figure 1 is presented the color variation of the solutions from light yellow to brown-orange, due to the different size distribution and concentration of the AgNPs.

The first characterization of the AgNPs solutions consisted in UV-VIS analysis. The UV-VIS spectra presented in Figure 2 revealed a difference in absorbance and wavelength

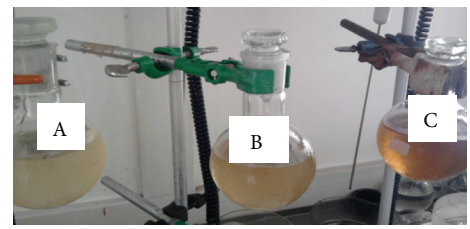

Figure 1: Samples A, B, and C of AgNPs solutions.

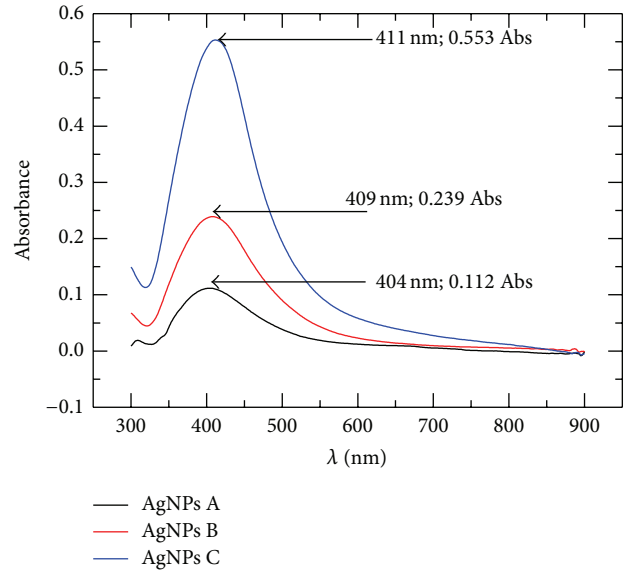

Figure 2: UV-VIS spectra of AgNPs solutions A, B, and C.

value. The wavelength value of the maximum absorption band is red-shifted between the samples which can be correlated with an increase of larger size particle content [21, 22]. Thus, sample A has the lowest values of both size and absorbance of AgNPs, followed by samples B and C, respectively.

DLS analysis was performed on the three solutions in order to obtain the mean diameter and size distribution of the AgNPs (Figure 3). For a more accurate size characterization, intensity and number of weighted mean diameters and distributions from DLS technique were considered. Although the whole range of diameters is shown in the intensity-weighted distribution (I-distribution), the proportionality to the sixth power of diameter of particle (D) ($I \propto D^6$) underestimates the small particles, which are only very weakly weighted [22, 23].

In the case of sample A, the DLS analysis revealed almost monodisperse AgNPs with a particle size range under 20 nm. From the DLS data, the weighted average diameter for sample A was estimated to be 12.6 nm. Sample B revealed two types of nanoparticles: the first presenting a weighted average diameter 13.6 nm while the second was calculated to be 83.6 nm. For sample C, the size polydispersity and weighted average diameter increased to around 24 nm with a small domain of larger particles. Thus, the main difference between

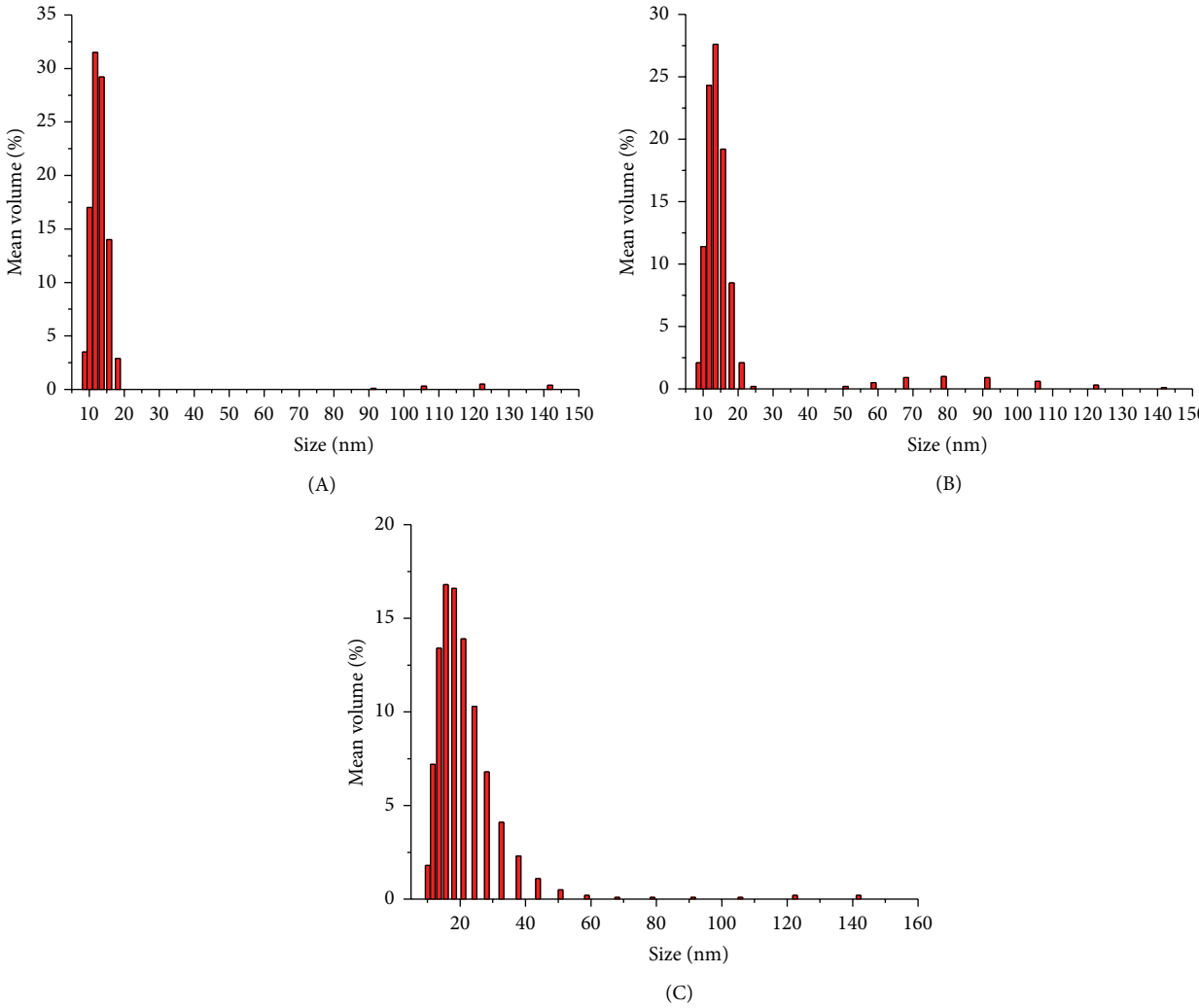

Figure 3: DLS analysis of A, B, and C AgNPs samples.

the three samples is the increase in polydispersity and particle size from A to C, in the order A < B < C, respectively, and the decrease in content of particles less than 20 nm.

In order to confirm the particles size, TEM analyses have been performed. In Figure 4 it can be noticed that the DLS data are sustained by TEM images.

The next step of this study was directed to the synthesis and investigation of the hybrid material (TiO_2 P25/AgNPs films). The images from Figure 5 present the color variation of TiO_2 P25, respectively, the hybrid TiO_2 P25/AgNPs films after the deposition and annealing process on a quartz tube. The color of the hybrid material can be explained by the addition of the reflected wavelength domain of TiO_2 P25 and AgNPs.

In order to characterize this color modification, the films obtained using TiO_2 P25 and the three AgNPs solutions (A, B, and C) were analyzed by UV-VIS (Figure 6). The obtained TiO_2 P25/AgNPs hybrid films registered different reflection bands compared with the reference (TiO_2 P25 film). The absorption bands are blue-shifted, while the AgNPs size distribution decreases (see inset). This can be explained by the overlaying of the adsorption bands of TiO_2 P25 film and different AgNPs particle size distribution. Thus, the registered signals are in good correlation with the results registered by DLS analysis (Figure 1) and UV-VIS analysis (Figure 1) of the initial AgNPs solutions.

The concentration of TiO_2 P25 is much higher than that of the AgNPs; therefore the spectroscopic influence of silver nanoparticles is rather minor on the UV-VIS absorption properties of the films; however, all the samples present absorption at a lower wavelength compared to the initial TiO_2 P25. Thus, the hybrid material is photoactive for a larger wavelength domain.

The photocatalytic activity of the hybrid nanocomposite films was determined using the experimental set-up presented in Scheme 2 (details on the procedure are presented in Section 2.4). The most important element of our experiment was the reactor equipped with the quartz tube and illuminated with an UV lamp.

The kinetics of photocatalytic degradation and the percentage of MO photodegraded are highly dependent on

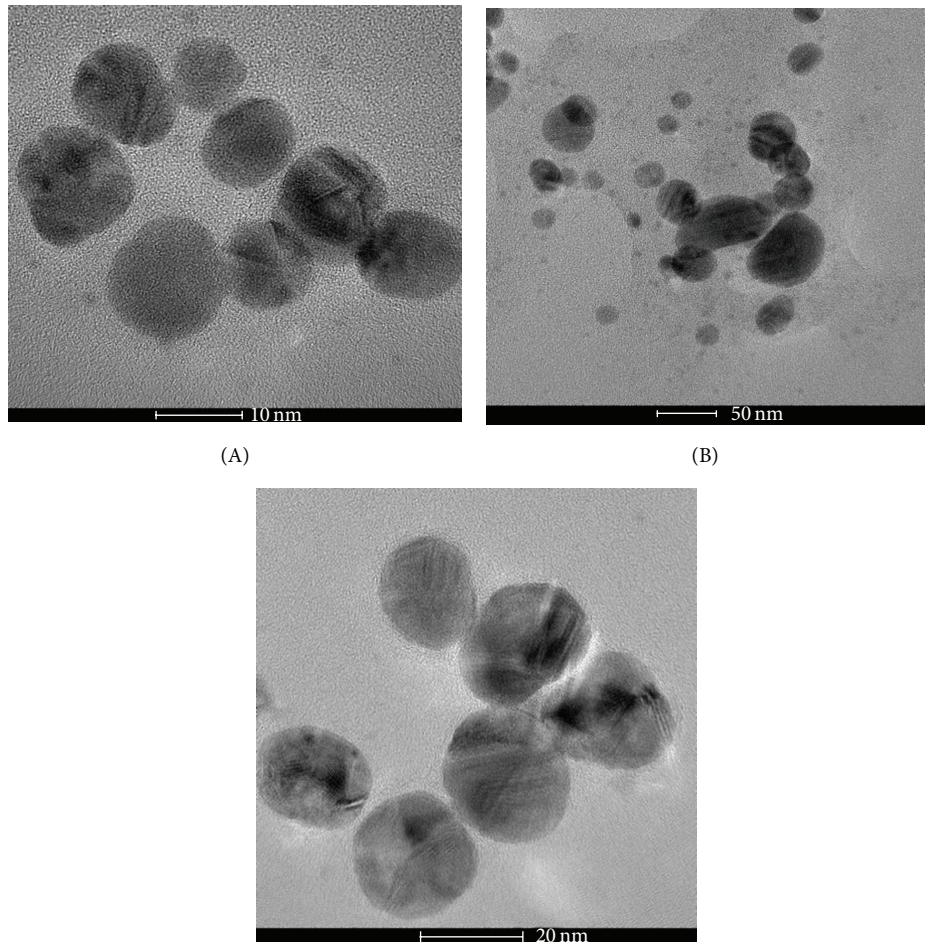

(A) (B)

(C)

Figure 4: TEM images for the samples A, B, and C.

AgNPs size. The highest photocatalytic activity was registered for the nanoparticles with the smallest size and narrower particle size distribution (sample A) (see DLS analysis, Figure 3).

Furthermore, in all three cases involving the hybrid materials, although the size of AgNPs nanoparticles increases, the photocatalytic activity registered superior values compared with the TiO_2 P25. Thus, after 150 min, the photodegradation percentage reaches 33%. The degradation curves are linear confirming a first order reaction degradation kinetics mechanism which allowed the utilization of the Langmuir-Hinshelwood model [24, 25] for determination of the apparent reaction constant (Figure 7). All the samples have presented adsorption characteristics similar to TiO_2 P25 for the "in the dark" study.

The analysis of the photodegradation results proved that the materials based on AgNPs improve the photoactivity of the TiO_2 films. The introduction of AgNPs in the TiO_2 P25 suspension increased the photodegradation of MO in all cases, regardless of the AgNPs size distribution.

For this reason, the next approach of this study aimed to increase the contact surface between TiO_2 P25 and AgNPs, simplifying the manufacturing process. Thus, in order to validate this method, AgNPs were generated directly on the surface of TiO_2 P25 film and the photoactivity of the obtained hybrid material was analyzed using MO.

In Figure 8, the SEM images of the TiO_2 P25 and for the new hybrid material are presented comparatively.

The SEM analysis reveals that AgNPs generated on the TiO_2 P25 surface form aggregates in different areas (Figure 7(b)) (red highlighted). Although their formation was preferential, the contact area with MO is enlarged and should register higher efficiency values.

The evolution of the decomposition process of the dye is presented in Figure 8. For a better investigation of the hybrid film, the results were compared with a simple TiO_2 P25 and the generated AgNPs/TiO_2 P25 film in the dark. From Figure 9, the film is very stable in the dark and the MO was not decomposed. The hybrid film resulting from the generation of AgNPs directly on TiO_2 P25 registered a photodegradation capacity of MO of 45% after 150 min.

This approach of reducing silver on the surface of TiO_2 P25 increased the direct contact of AgNPs with the contaminated medium which determined a higher efficiency of

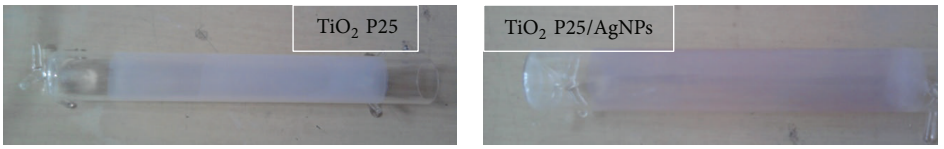

Figure 5: Images of TiO_2 P25 and TiO_2 P25/AgNPs films after deposition and annealing on the quartz tube.

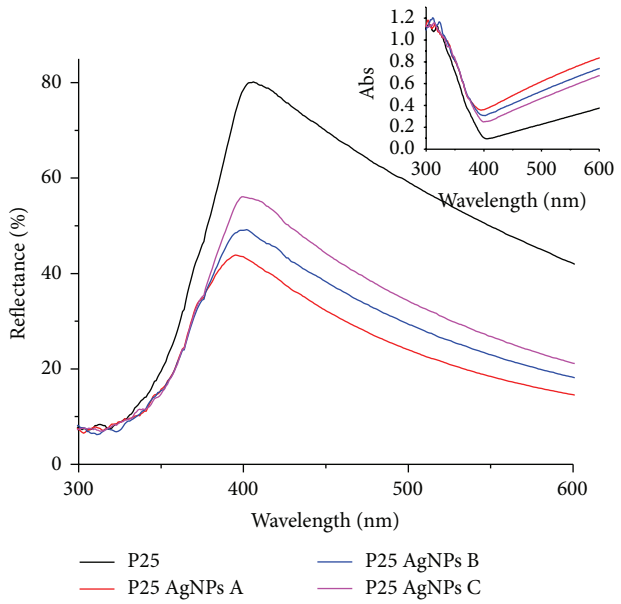

Figure 6: The UV-VIS spectra of the hybrid films.

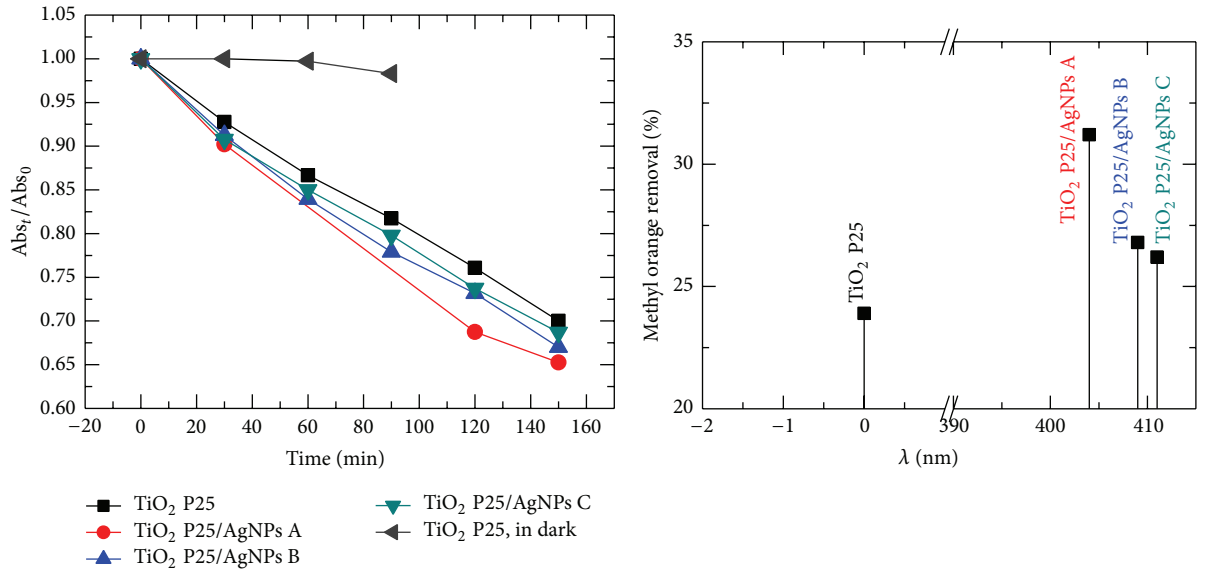

(a) (b)

Sample	TiO_2 P25	A	B	C
The apparent decomposition constant (k_{app}) (min^{-1})	21.0×10^{-4}	31×10^{-4}	26.1×10^{-4}	24.6×10^{-4}

(c)

Figure 7: (a) Photodegradation kinetics; (b) percentage of decomposed MO versus maximum absorption wavelength value of the AgNPs solution; (c) values of apparent decomposition constant.

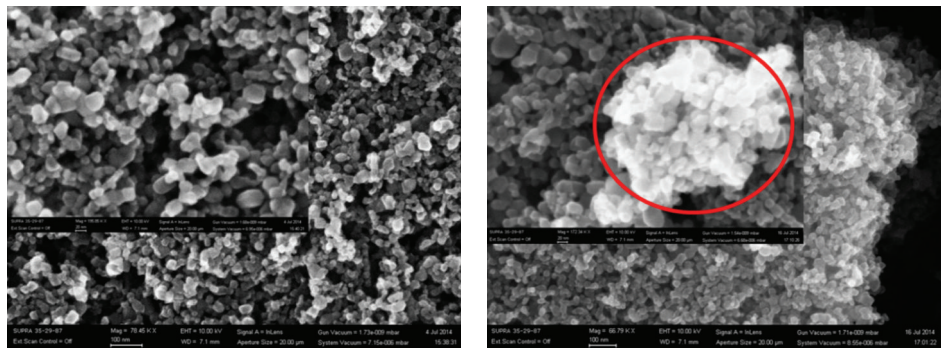

(a) (b)

Figure 8: SEM images of TiO_2 P25 (a) and AgNPs generated on the surface of TiO_2 P25 (b).

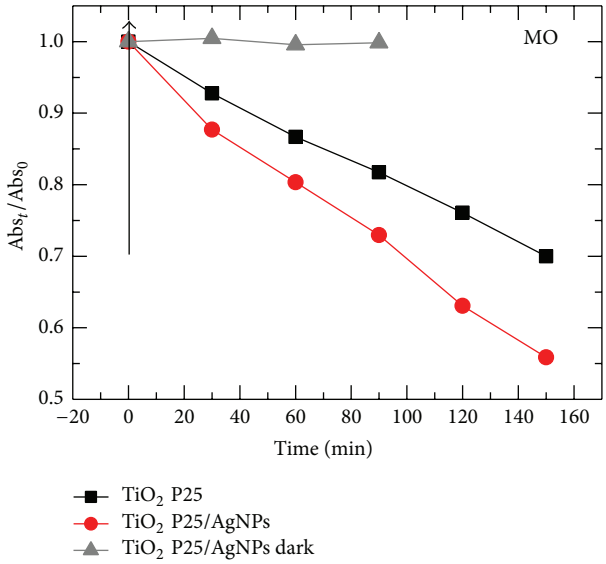

Figure 9: The photodegradation evolution of MO in the presence of AgNPs generated directly on TiO_2 P25 film.

the degradation process, sustaining also the possible photodegradation mechanism of the dye.

4. Conclusions

The aim of the present study consisted in the obtaining of hybrid material films, using TiO_2 P25 and AgNPs. In the first case (mixing TiO_2 P25 with AgNPs solutions), the size distribution of the AgNPs proved to be a key element in the photodegradation activity of the materials; the main difference between the three samples is the increase in polydispersity and particle size from A to C, in the order A < B < C, respectively, and the decrease in content of particles less than 20 nm. For the first case, the degradation of MO is about 33% after 150 min under UV irradiation.

The second approach involved the generation of AgNPs on the surface of the TiO_2 P25 film. In this case, the contact surface of AgNp with MO is higher and the photodegradation activity increased to 45% after 150 min.

Conflict of Interests

The authors Tomkouani Kodom, Edina Rusen, Ioan Călinescu, Alexandra Mocanu, Raluca Şomoghi, Adrian Dinescu, Aurel Diacon, and Cristian Boscornea declare that there is no conflict of interests regarding the publication of this paper.

Acknowledgments

Tomkouani Kodom would like to thank the postdoctoral Scholarships Programme "Eugen Ionescu" of the Francophony University Agency (AUF) for financial support. Aurel Diacon and Alexandra Mocanu acknowledge financial support from the Sectoral Operational Programme Human Resources Development 2007–2013 of the Ministry of European Funds through the Financial Agreements POSDRU/159/1.5/S/132395 and POSDRU/159/1.5/S/132397.

References

[1] S. Malato, P. Fernández-Ibáñez, M. I. Maldonado, J. Blanco, and W. Gernjak, "Decontamination and disinfection of water by solar photocatalysis: recent overview and trends," *Catalysis Today*, vol. 147, no. 1, pp. 1–59, 2009.

[2] M. A. Shannon, P. W. Bohn, M. Elimelech, J. G. Georgiadis, B. J. Marîas, and A. M. Mayes, "Science and technology for water purification in the coming decades," *Nature*, vol. 452, no. 7185, pp. 301–310, 2008.

[3] J. Qiu, S. Zhang, and H. Zhao, "Recent applications of TiO_2 nanomaterials in chemical sensing in aqueous media," *Sensors and Actuators B: Chemical*, vol. 160, no. 1, pp. 875–890, 2011.

[4] M. A. Nawi and S. M. Zain, "Enhancing the surface properties of the immobilized Degussa P-25 TiO_2 for the efficient photocatalytic removal of methylene blue from aqueous solution," *Applied Surface Science*, vol. 258, no. 16, pp. 6148–6157, 2012.

[5] M. A. Henderson, "A surface science perspective on TiO_2 photocatalysis," *Surface Science Reports*, vol. 66, no. 6-7, pp. 185–297, 2011.

[6] X. Zhang, Y. Wang, and G. Li, "Effect of operating parameters on microwave assisted photocatalytic degradation of azo dye X-3B with grain TiO_2 catalyst," *Journal of Molecular Catalysis A: Chemical*, vol. 237, no. 1-2, pp. 199–205, 2005.

[7] U. G. Akpan and B. H. Hameed, "Parameters affecting the photocatalytic degradation of dyes using TiO_2-based photocatalysts: a review," *Journal of Hazardous Materials*, vol. 170, no. 2-3, pp. 520–529, 2009.

[8] F. Hossain, O. J. Perales-Perez, S. Hwang, and F. Román, "Antimicrobial nanomaterials as water disinfectant: applications, limitations and future perspectives," *Science of the Total Environment*, vol. 466-467, pp. 1047–1059, 2014.

[9] Y. Chen and D. D. Dionysiou, "Effect of calcination temperature on the photocatalytic activity and adhesion of TiO_2 films prepared by the P-25 powder-modified sol-gel method," *Journal of Molecular Catalysis A: Chemical*, vol. 244, no. 1-2, pp. 73–82, 2006.

[10] T. Sreethawong, S. Ngamsinlapasathian, and S. Yoshikawa, "Positive role of incorporating P-25 TiO_2 to mesoporous-assembled TiO_2 thin films for improving photocatalytic dye degradation efficiency," *Journal of Colloid and Interface Science*, vol. 430, pp. 184–192, 2014.

[11] A. L. Linsebigler, G. Lu, and J. T. Yates Jr., "Photocatalysis on TiO_2 surfaces: principles, mechanisms, and selected results," *Chemical Reviews*, vol. 95, no. 3, pp. 735–758, 1995.

[12] L. Liu, J. Yang, S. Liu et al., "Hollow hybrid titanate/Au@TiO_2 hierarchical architecture for highly efficient photocatalytic application," *Catalysis Communications*, vol. 54, pp. 66–71, 2014.

[13] S. Niyomkarn, T. Puangpetch, and S. Chavadej, "Mesoporous-assembled In2O3-TiO_2 mixed oxide photocatalysts for efficient degradation of azo dye contaminant in aqueous solution," *Materials Science in Semiconductor Processing*, vol. 25, pp. 112–122, 2014.

[14] Y. Bessekhouad, R. Brahimi, F. Hamdini, and M. Trari, "Cu_2S/TiO_2 heterojunction applied to visible light Orange II degradation," *Journal of Photochemistry and Photobiology A: Chemistry*, vol. 248, pp. 15–23, 2012.

[15] H. Feng, T. Tran, L. Chen, L. Yuan, and Q. Cai, "Visible light-induced efficiently oxidative decomposition of p-Nitrophenol by CdTe/TiO_2 nanotube arrays," *Chemical Engineering Journal*, vol. 215-216, pp. 591–599, 2013.

[16] M. K. Seery, R. George, P. Floris, and S. C. Pillai, "Silver doped titanium dioxide nanomaterials for enhanced visible light photocatalysis," *Journal of Photochemistry and Photobiology A: Chemistry*, vol. 189, no. 2-3, pp. 258–263, 2007.

[17] Q. Li, S. Mahendra, D. Y. Lyon et al., "Antimicrobial nanomaterials for water disinfection and microbial control: potential applications and implications," *Water Research*, vol. 42, no. 18, pp. 4591–4602, 2008.

[18] B. Tian, R. Dong, J. Zhang, S. Bao, and F. Yang, "Sandwich-structured AgCl at Ag at TiO_2 with excellent visible-light photocatalytic activity for organic pollutant degradation and *E. coli* K12 inactivation," *Applied Catalysis B: Environmental*, vol. 158-159, pp. 76–84, 2014.

[19] J. Xu, X. Xiao, F. Ren et al., "Enhanced photocatalysis by coupling of anatase TiO_2 film to triangular Ag nanoparticle island," *Nanoscale Research Letters*, vol. 7, article 239, 2012.

[20] J. Gamage McEvoy and Z. Zhang, "Antimicrobial and photocatalytic disinfection mechanisms in silver-modified photocatalysts under dark and light conditions," *Journal of Photochemistry and Photobiology C: Photochemistry Reviews*, vol. 19, no. 1, pp. 62–75, 2014.

[21] T. Dadosh, "Synthesis of uniform silver nanoparticles with a controllable size," *Materials Letters*, vol. 63, no. 26, pp. 2236–2238, 2009.

[22] E. Tomaszewska, K. Soliwoda, K. Kadziola et al., "Detection limits of DLS and UV-Vis spectroscopy in characterization of polydisperse nanoparticles colloids," *Journal of Nanomaterials*, vol. 2013, Article ID 313081, 10 pages, 2013.

[23] S. U. Egelhaaf, E. Wehrli, M. Müller, M. Adrian, and P. Schurtenberger, "Determination of the size distribution of lecithin liposomes: a comparative study using freeze fracture, cryo-electron microscopy and dynamic light scattering," *Journal of Microscopy*, vol. 184, no. 3, pp. 214–228, 1996.

[24] A. Houas, H. Lachheb, M. Ksibi, E. Elaloui, C. Guillard, and J.-M. Herrmann, "Photocatalytic degradation pathway of methylene blue in water," *Applied Catalysis B: Environmental*, vol. 31, no. 2, pp. 145–157, 2001.

[25] Z. Zainal, L. K. Hui, M. Z. Hussein, A. H. Abdullah, and I. R. Hamadneh, "Characterization of TiO_2-chitosan/glass photocatalyst for the removal of a monoazo dye via photodegradation-adsorption process," *Journal of Hazardous Materials*, vol. 164, no. 1, pp. 138–145, 2009.